Phonon Spectromicroscopy of Carbon Nanostructures with Atomic Resolution

L. Vitali,[1] M. Burghard,[1] M. A. Schneider,[1] Lei Liu,[2] S. Y. Wu,[2] C. S. Jayanthi,[2] and K. Kern[1]

[1]*Max-Planck Institut für Festkörperforschung, Heisenbergstrasse 1, D-70569 Stuttgart, Germany*
[2]*Department of Physics, University of Louisville, Louisville, Kentucky 40292, USA*

The vibrational properties of single-wall carbon nanotubes have been probed locally with atomic-scale resolution by inelastic electron tunneling spectroscopy with a low-temperature scanning tunneling microscope. The high spatial resolution has allowed the unraveling of changes in the local phonon spectrum related to topological defects. We demonstrated that the radial breathing mode is suppressed within tube segments of lengths below ~3 nm, and that in the cap region phonon modes characteristic of the fullerene hemisphere are emerging. Phonon spectromicroscopy should lead to a better understanding of the mechanisms that limit the transport of heat or electrical charge inside nanostructured carbon materials.

The physical properties of carbon nanostructures critically depend on the local molecular structure and bonding, a sensitive fingerprint of which is the local vibrational density of states [1]. A means of characterizing the vibrational spectra with high spatial resolution and sensitivity is therefore highly desirable. Optical techniques have insufficient spatial resolution to explore the local vibrational features of carbon nanotubes on the relevant subnanometer scale [2–4]. Here we demonstrate the use of inelastic electron tunneling spectroscopy with a low-temperature scanning tunneling microscope to probe the vibrational modes of carbon nanotubes with ultimate spatial resolution. The radial breathing mode (RBM) of individual carbon nanotubes adsorbed on Au(111) is detected locally, and the linear dependence of the RBM vibrational energy on the inverse of the tube diameter is proven. Most importantly, we demonstrate the sensitivity of the phonon mode to topological defects by mapping its frequency with atomic spatial resolution across an intramolecular junction and a tube cap.

Local probe techniques, such as scanning tunneling microscopy (STM), have successfully been applied to study the electronic structure of single-wall carbon nanotubes (SWCNTs) [5–7]. Native and intentionally introduced defects have been observed experimentally [5,6,8–10]. Although these local geometric and electronic structures have been well characterized, their signature in the vibrational spectrum is largely unknown both experimentally and theoretically. Probing the local vibrational density of states is, however, becoming accessible through inelastic electron tunneling spectroscopy (IETS) using a scanning tunneling microscope. A few percent of the electrons tunneling through the STM vacuum junction scatter inelastically, exciting a vibration of the sample under investigation [11], which is detected in the second derivative of the tunneling current d^2I/dV^2. IETS-STM is therefore an ideal tool for the local vibrational spectroscopy of nanostructures. The technique has been pioneered by Ho and collaborators focusing on the spectroscopy of localized vibrations of single molecules adsorbed on metallic surfaces [12]. Very elegant experiments have addressed adsorbed molecules ranging in size from acetylene to C_{60} [12,13]. The detection of collective vibrations as surface phonons with this technique was reported earlier [14], but only recently it could be demonstrated that in the case of a graphite surface the IETS-STM spectrum is directly proportional to the total density of phonon states [15]. The phonon modes of the graphite surface could be determined with high accuracy, naturally suggesting the application of IETS-STM to confined geometries and individual carbon nanostructures.

In the experiments reported here, as-produced HiPco material (tubes@Rice) has been ultrasonically dispersed in 1,2-dichloroethane and deposited on Au/mica substrates as described in Ref. [7]. The samples have been transferred into an ultra high vacuum system equipped with a home-built STM, and tunneling experiments performed at 6 K using a tungsten tip. More than 20 individual tubes have been selected and identified according to their chiral index (n, m), which defines the chiral vector of the tubes. For the latter purpose, a method reported by Wildöer *et al.* [16] was followed. Specifically, the separation of the van Hove singularities (vHs) in the electronic local density of states (LDOS) was used to determine the diameter of metallic and semiconducting tubes [17]. In addition, the chiral angle was obtained from atomically resolved STM images.

The inelastic spectra obtained on different isolated tubes revealed several energy loss features ranging from the RBM to the *G* band (200 meV). These showed the symmetry of the losses with respect to electron or hole tunneling, expected for inelastic excitations in IETS-STM technique. In the following, we focus on the low-energy region which contains the RBM. Being intensively studied and showing a pronounced sensitivity to the local environment, the RBM is the ideal candidate to probe the influence of local structures on the vibrational features.

The low-energy IETS-STM spectra of eight different isolated SWCNTs, taken over topographically clean and defect free tube surfaces, are displayed in Fig. 1(a). Each spectrum exhibits one prominent peak, and the voltage position of the peaks is observed to decrease with the magnitude of the chiral indices, i.e., with an increase in tube diameter. To clarify the nature of these vibrations, the peak energy is plotted in Fig. 1(b) as a function of inverse tube diameter (solid squares). The observation of phonon energies in the range of 10–30 meV and the inverse scaling of phonon energy with tube diameter (d_t) show that the peaks originate from excitation of the RBM in the tubes.

Further support for the assignment of the peaks to the RBM is gained by a comparison of experimental measurements with theoretically calculated phonon energies based on a sp^3 nonorthogonal tight-binding (NOTB) Hamiltonian [18]. In the present calculation, first equilibrium configurations of tubes of different chiralities that fall within the experimentally relevant diameter range (0.7–3 nm) are determined by molecular dynamics, and then the force constant matrices for each of these relaxed configurations are evaluated numerically [19]. The calculated RBM frequencies for the same set of eight nanotubes [as shown in Fig. 1(a)] are plotted against inverse diameter of the tube as open circles in Fig. 1(b). The RBM energies obey the relation $E_{RBM} = A/d_t$, where $A =$

262 meV Å. It can also be seen that this relationship describes the measured phonon energies very well. The coefficient A is found to be in general agreement with values obtained by other theoretical calculations, such as the force constant model [20], the zone-folding method [21], density functional theories based on plane wave basis sets [22], and pseudoatomic orbitals [23]; they lie in the range of 270–292 meV Å. This result confirms that the NOTB approach is able to appropriately predict the vibrational properties of SWCNTs.

Having established that IETS-STM allows for atomic-scale spectroscopy of vibrations in SWCNTs, we extended our studies towards detecting changes in the vibrational structure that arises from the presence of defects. Of special interest in this respect are intramolecular junctions connecting two different tubes, which require at least one pentagon-heptagon pair [6,24,25], and the highly curved tube caps containing at least six pentagons [9,26]. Figure 2(a) shows the topographic image of an isolated metallic (17,14) tube, which was selected for detailed spectroscopic investigations since it combines both of these features. The presence of an intramolecular junction is visible at a distance of ~5 nm from the tube apex, where the tube diameter abruptly decreases from 21.2 to 9.7 Å while the chiral angle is preserved. The short tube segment (denoted as the "neck region") that follows behind the junction is attributed to either a (8,6) or a (8,7) tube, both of which are semiconductors. The neck region reaches a length of 2 nm, where it gets closed by an apparently intact cap ("cap region").
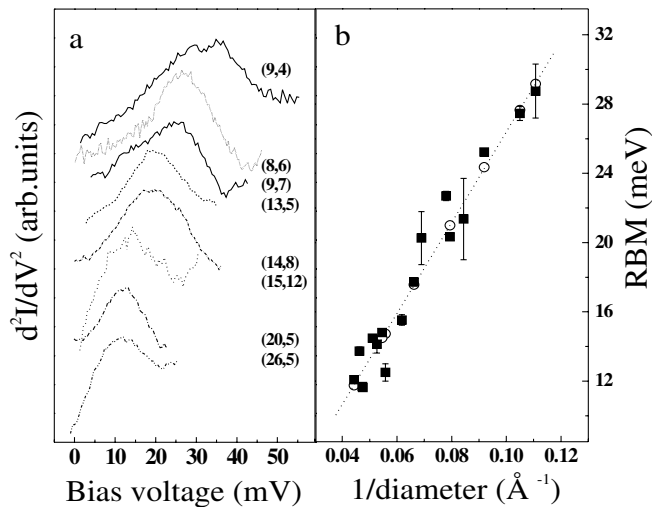

FIG. 1. (a) IETS-STM spectra of eight different isolated SWCNTs, obtained at 6 K as the d^2I/dV^2 lock-in signal with a bias modulation of 10 meV at a frequency of 2.7 kHz in the energy range of the RBM. Each spectrum is labeled by the (n, m) pair of the respective tube. The spectra have been arranged such that the tube diameter increases from the top to the bottom. (b) Energy of the RBM of isolated SWCNTs plotted against the inverse diameter. The experimentally observed peak energies in the IETS and the theoretically calculated phonon energies are shown as solid squares and open circles, respectively.
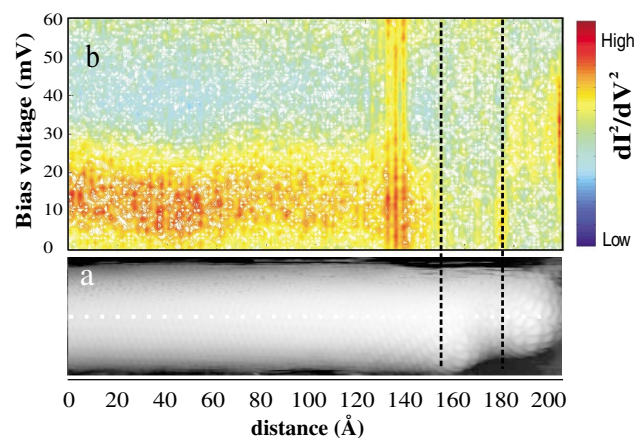

FIG. 2 (color). Changes in the local vibrational properties of a SWCNT associated with the presence of local defects. (a) Topographic image of a (17,14) tube containing an intramolecular tube junction and a closed ending. The transitions between the corresponding regions are highlighted by black dashed lines. The white dotted line indicates the sampling positions along the tube axis where the IETS spectra were taken. (b) Color scale map of the lock-in signal (d^2I/dV^2) as a function of energy and position along the tube axis.
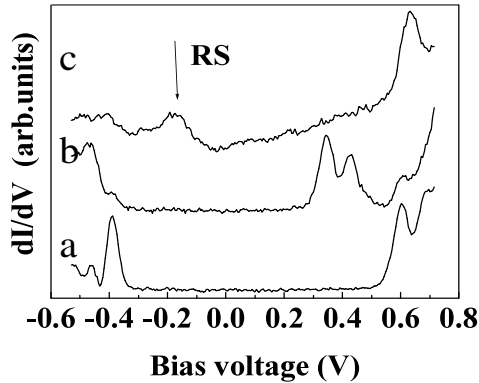
FIG. 3. Scanning tunneling spectra displaying the electronic LDOS at different regions of the (17,14) tube depicted in Fig. 2(a). The spectra were acquired at the tube body (spectrum *a*), the neck region (spectrum *b*), and the tube cap (spectrum *c*). The electronic LDOS at the cap exhibits a peak at ~ -0.2 V, which is attributed to a resonant state (RS).

The structural changes deduced from an inspection of the topographic image are further corroborated by the simultaneously acquired electronic LDOS, which are depicted in Fig. 3 for the three different tubes regions. The differential conductance spectrum recorded on the (17,14) tube shows the characteristics of a metallic tube. Upon moving to the neck region, the separation between the first pair of vHs decreases despite the decreased tube diameter, indicating that the electronic character has changed from metallic to semiconducting. Finally, when the cap is reached, an additional differential conductance peak has developed inside the gap region. This peak (labeled RS) is ascribed to a resonant state in the cap, which has been predicted by theory [26,27] and experimentally observed at the closed ending of another type of tube [5,9,10].

The IETS-STM spectra measured as a function of position along the (17,14) tube [indicated as white dotted line in Fig. 2(a)] are displayed in Fig. 2(b) as a color map. This set of spectra was acquired by sampling the tube each ~ 1.5 Å. On top of the (17,14) tube, the RBM is found at a constant energy of ~ 12 meV, in close agreement with the value obtained from theory [see Fig. 2(b)]. One further observes the abrupt disappearance of this RBM at the intramolecular junction. Although one would expect a RBM to occur at 25 meV in the neck region according to its diameter, no such mode is evident. However, when the cap region is reached, a new vibrational feature appears at 29 meV.

Since it is computationally not feasible to study the dynamics of a (17,14) tube fused to a (8,7) or a (8,6) tube and terminated by a cap due to its system size, we chose to carry out the dynamics of low-energy vibrations of a (5,5) tube capped by C_{60} hemispheres at both ends to delineate the following issues: (i) What is the effect of the cap on the RBM associated with the tube? (ii) Can the RBM associated with the cap be observed in the experiment? (iii) What is the effect of the length of the tube on the RBM? (iv) Can the "RBM" be sustained in short tubes? Our calculations of the eigenfrequencies and eigendisplacements for relaxed structures of (5,5) capped tubes of different lengths up to 40 nm revealed that the tube is able to sustain a RBM only if its length exceeds 3.5 nm. This phonon mode is identified as a RBM because its eigendisplacement has a nonzero radial and a zero tangential component. In the 40 nm-long tube, the radial displacement is found to exhibit a spatially oscillating pattern in the tube region, which arises from the finite length. Similar results were reported in a study of finite-size effects in SWCNTs with free open ends, i.e., without cap terminations [28]. In the present case, a pronounced influence of the caps is apparent from the fact that the radial displacement abruptly drops to zero in their proximity. The RBM has a frequency of ~ 39 meV, in close agreement with the value calculated from $E_{RBM} = 262$ meV Å$/d_t$ for an infinite-length (5,5) tube.

Our calculation also reveals a cap-specific phonon mode at $\omega = 59$ meV whose energy is close to that of the RBM of a C_{60} molecule. As shown in Fig. 4, this mode has nonzero radial displacement and zero tangential displacement in the cap region, akin to the RBM of a C_{60}. However, the character of this mode is transformed from a pure radial nature to a tangential-dominant character in the tube (bulk) region. This is the consequence of the resonance between the RBM of the hemispherical C_{60} cap and a bulk mode of the tube.
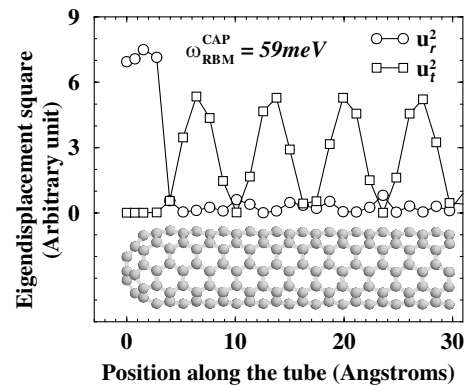

FIG. 4. Eigenvector characteristics of a cap-specific eigenmode at ~ 59 meV in a finite-length (40 nm) carbon nanotube capped by C_{60} hemispheres. This mode has finite radial (u_r) and zero tangential (u_t) displacements in the cap region (0–3.5 Å), akin to the characteristics of the RBM of a molecule. The nature of this mode transforms from a radial to a tangential character in the interior of the tube, a consequence of the resonance between the RBM of the C_{60} hemispherical cap and a bulk mode.

Although our theoretical calculation for the (5,5) capped nanotube cannot capture the "defect modes" due to the intertube junction, it can still provide a scenario or general guidelines for the dynamics of any capped nanotube, in particular, the effect of the cap and the finiteness of the tube on the RBM. For example, we predict that, in the tube region, the RBM will be observed if its length is sufficiently large. Furthermore, it will occur at the same frequency as that of an infinite tube, if there is no hybridization between the RBM of the tube and the cap-specific mode. However, if the tube length is short, it cannot sustain the RBM. Hence, we predict that the RBM will not manifest in the neck region for the experimental sample, since its length is too short. This scenario is completely reflected by the experimental observations on the capped (17,14) tube shown in Fig. 2: (i) In the tube region, the experimentally observed RBM occurs at ~ 12 meV, consistent with the theoretically calculated frequency (12.6 meV) of the RBM of an infinite (17,14) tube. (ii) In the neck region, there is no observation of a RBM because of the shortness of the neck (~ 2 nm). (iii) In the cap region, a mode at 29 meV was experimentally observed, akin to the theoretically predicted resonance mode between the RBM of the cap and a bulk mode. Since the calculated RBM frequencies of C_{140} (with the radius of 5.4 Å) and C_{240} (with the radius of 7.0 Å) are found to be ~ 43 meV and ~ 25 meV, respectively, the experimentally observed 29 meV cap mode suggests that the radius of curvature of the cap may be estimated to be ~ 6 Å.

In conclusion, STM-based IETS has been demonstrated to offer experimental access to the vibrational properties of SWCNTs on the molecular scale. Its ability to simultaneously detect the molecular structure and the vibrational features of a given nanotube, which distinguish this technique from other methods, has allowed us to demonstrate unequivocally the theoretically predicted relation of the tube diameter and RBM frequency. Furthermore, our data show for the first time the dependence of vibrational properties on structural changes as the suppression of the RBM in close proximity to a defect site, or inside isolated tube segments with lengths of the order of a few nanometers. For future studies, STM-IETS offers the unique possibility to correlate local vibrational changes arising from various types of tube modifications with the local electronic structure. For instance, the study of tube deformations such as kinks or twists could deepen the understanding of the effect of stress fields on the electrical transport properties of SWCNTs.

[1] M. S. Dresselhaus, G. Dresselhaus, and P. C. Eklund, *Science of Fullerenes and Carbon Nanotubes* (Academic Press, New York, 1996).
[2] A. Mews *et al.*, Adv. Mater. **12**, 1210 (2000).
[3] B. Knoll and F. Keilmann, Nature (London) **399**, 134 (1999).
[4] A. Hartschuh *et al.*, Phys. Rev. Lett. **90**, 095503 (2003).
[5] D. L. Carroll *et al.*, Phys. Rev. Lett. **78**, 2811 (1997).
[6] M. Ouyang *et al.*, Science **291**, 97 (2001).
[7] L. C. Venema *et al.*, Phys. Rev. B **61**, 2991 (2000).
[8] H. Kim *et al.*, Phys. Rev. Lett. **90**, 216107 (2003).
[9] P. Kim *et al.*, Phys. Rev. Lett. **82**, 1225 (1999).
[10] Z. Klusek, P. Kowalczyk, and P. Byszewski, Vacuum **63**, 145 (2001).
[11] N. Lorente and M. Persson, Phys. Rev. Lett. **85**, 2997 (2000).
[12] B. C. Stipe, M. A. Rezaei, and W. Ho, Science **280**, 1732 (1998).
[13] J. I. Pascual *et al.*, J. Chem. Phys. **117**, 9531 (2002).
[14] D. P. E. Smith, G. Binnig, and C. F. Quate, Appl. Phys. Lett. **49**, 1641 (1986).
[15] L. Vitali *et al.*, Phys. Rev. B **69**, 121414(R) (2004).
[16] J. W. G. Wildöer *et al.*, Nature (London) **391**, 59 (1998).
[17] The distance between the vHs is related to tube diameter by $E = b\gamma_0 a_{C-C}/d$, where b is a constant equal to two for semiconducting tubes and to six for metallic ones, γ_0 is the nearest neighbor tight-binding overlap energy (assumed to be 2.5 eV), a_{C-C} is the nearest neighbor distance, and d is the tube diameter.
[18] M. Menon, E. Richter, and K. R. Subbaswamy, J. Chem. Phys. **104**, 5875 (1996).
[19] L. Liu, C. S. Jayanthi, and S. Y. Wu, Phys. Rev. B **68**, 201301(R) (2003).
[20] A. M. Rao *et al.*, Science **275**, 187 (1997).
[21] R. A. Jishi *et al.*, Chem. Phys. Lett. **209**, 77 (1993).
[22] J. Kürti, G. Kresse, and H. Kuzmany, Phys. Rev. B **58**, R8869 (1998).
[23] D. Sánchez-Portal *et al.*, Phys. Rev. B **59**, 12678 (1999).
[24] R. Saito, G. Dresselhaus, and M. S. Dresselhaus, Phys. Rev. B **53**, 2044 (1996).
[25] H. J. Choi, J. Ihm, S. G. Louie, and M. L. Cohen, Phys. Rev. Lett. **84**, 2917 (2000).
[26] T. Yaguchi and T. Ando, J. Phys. Soc. Jpn. **71**, 2224 (2002).
[27] Y. Kasahara, R. Tamura, and M. Tsukada, Phys. Rev. B **67**, 115419 (2003).
[28] R. Saito *et al.*, Phys. Rev. B **59**, 2388 (1999).